

# Accurate detection of hierarchical communities in complex networks based on nonlinear dynamical evolution

Zhao Zhuo, Shi-Min Cai, Ming Tang, and Ying-Cheng Lai

Citation: *Chaos* **28**, 043119 (2018); doi: 10.1063/1.5025646

View online: <https://doi.org/10.1063/1.5025646>

View Table of Contents: <http://aip.scitation.org/toc/cha/28/4>

Published by the [American Institute of Physics](#)

---

---

**PHYSICS TODAY**

WHITEPAPERS

**ADVANCES IN PRECISION  
MOTION CONTROL**

Piezo Flexure Mechanisms  
and Air Bearings

READ NOW

PRESENTED BY

**PI**

## Accurate detection of hierarchical communities in complex networks based on nonlinear dynamical evolution

Zhao Zhuo,<sup>1,2</sup> Shi-Min Cai,<sup>1,3,a)</sup> Ming Tang,<sup>3,4</sup> and Ying-Cheng Lai<sup>5</sup>

<sup>1</sup>Web Sciences Center, School of Computer Science and Engineering, University of Electronic Science and Technology of China, Chengdu 611731, China

<sup>2</sup>College of Communication and Electronic Engineering, Qingdao University of Technology, Qiangdao 266520, China

<sup>3</sup>Institute of Fundamental and Frontier Sciences and Big Data Research Center, University of Electronic Science and Technology of China, Chengdu 611731, China

<sup>4</sup>School of Information Science Technology, East China Normal University, Shanghai 200241, China

<sup>5</sup>School of Electrical Computer and Energy Engineering, Arizona State University, Tempe, Arizona 85287, USA

(Received 12 February 2018; accepted 2 April 2018; published online 25 April 2018)

One of the most challenging problems in network science is to accurately detect communities at distinct hierarchical scales. Most existing methods are based on structural analysis and manipulation, which are NP-hard. We articulate an alternative, dynamical evolution-based approach to the problem. The basic principle is to computationally implement a nonlinear dynamical process on all nodes in the network with a general coupling scheme, creating a networked dynamical system. Under a proper system setting and with an adjustable control parameter, the community structure of the network would “come out” or emerge naturally from the dynamical evolution of the system. As the control parameter is systematically varied, the community hierarchies at different scales can be revealed. As a concrete example of this general principle, we exploit clustered synchronization as a dynamical mechanism through which the hierarchical community structure can be uncovered. In particular, for quite arbitrary choices of the nonlinear nodal dynamics and coupling scheme, decreasing the coupling parameter from the global synchronization regime, in which the dynamical states of all nodes are perfectly synchronized, can lead to a weaker type of synchronization organized as clusters. We demonstrate the existence of optimal choices of the coupling parameter for which the synchronization clusters encode accurate information about the hierarchical community structure of the network. We test and validate our method using a standard class of benchmark modular networks with two distinct hierarchies of communities and a number of empirical networks arising from the real world. Our method is computationally extremely efficient, eliminating completely the NP-hard difficulty associated with previous methods. The basic principle of exploiting dynamical evolution to uncover hidden community organizations at different scales represents a “game-change” type of approach to addressing the problem of community detection in complex networks. *Published by AIP Publishing.*

<https://doi.org/10.1063/1.5025646>

A ubiquitous feature of complex networks in the real world is a modular or a community structure, where nodes are organized into sparsely linked groups with dense connections within each group. The problem of detecting the modular structure without knowledge such as the number of communities is an non-deterministic polynomial hard (NP-hard) problem. Most existing methods of community detection rely on network structure analysis and manipulation. Our work is motivated by the interplay between the network structure and dynamics. In spite of the large body of literature on the effect of the network structure on collective dynamics, studies in the opposite direction, i.e., how network dynamics reveal the network structure, are relatively rare. Our idea is then to exploit network evolution dynamics to solve the challenging problem of hierarchical community detection. We demonstrate that it is indeed feasible to achieve accurate detection of communities in complex networks through clustered synchronization

dynamics. Given a network whose modular structure is to be deciphered, we implement nonlinear oscillatory nodal dynamics and systematically vary the coupling parameter. We show that for proper values of the coupling parameter, synchronous clusters at different scales emerge, which naturally reveal the hierarchical community structure of the network. That is, by tuning the coupling parameter, one can obtain the hierarchical community structure at different scales through simple observation of the network synchronization dynamics. The emergence and evolution of clustered synchronization can be analyzed by the standard method of master stability function (MSF). The analysis reveals the existence of distinct parameter intervals in which the synchronous clusters correspond exactly to the community structure at a particular scale. Combining information from all the parameter intervals provides an accurate picture of the hierarchical community structure of the network. We validate the dynamical evolution based approach using a benchmark network with adjustable intra- and inter-community linkage and test it on a number

<sup>a)</sup>Electronic mail: csm1981@mail.ustc.edu.cn

of real world networks. Our work represents a “game-change” type of principle to address the problem of network community detection.

## I. INTRODUCTION

It is common for complex networks in the real world to possess a modular or a community structure, where distinct groups of nodes emerge with the characteristic that the links within any individual group (community) are dense, whereas inter-group linkage is sparse.<sup>1</sup> Given a network, the number of possible communities is often not known *a priori* and, even if known, their sizes are typically different. Under such circumstances, to determine whether there are indeed communities and, for each and every node, the community that it belongs to is an computationally extremely challenging problem, making the detection of communities an NP-hard problem.<sup>2,3</sup> Since the community structure represents a fundamental organization of the network at the system level, to accurately detect communities is critical to understanding the functions, collective dynamics, and vulnerabilities of the underlying network, as well as to articulation of control strategies. The community detection problem is thus of great importance to a number of disciplines in which complex networks arise, such as biological, social, and computer sciences, and has been an active area of research in modern network science and engineering.

Most existing methods of detecting communities are based on network structure analysis and manipulation. The seminal work in this area is the Girvan-Newman algorithm,<sup>1</sup> which exploits the betweenness centrality<sup>4</sup> to identify the inter-community links and then removes them, so that the end result is a number of isolated communities. The computation overload of this method is, however, quite high, limiting its practical usage to small networks.<sup>5</sup> Another intuitive method is based on the idea of minimum cut,<sup>6</sup> where the network is divided into a number of groups of approximately equal size with the goal of seeking the optimal division so as to minimize the number of links among the groups. The methodology finds applications in parallel computing to balance load to minimize communication between a large number of Central Processing Unit (CPU) nodes. A widely used method is modularity maximization,<sup>5,7–12</sup> which identifies communities by varying the division of a network into groups and seeking the one that maximizes modularity (a measure characterizing the “quality” of a division) through procedures such as greedy algorithm, spectral optimization, and simulated annealing. A recent method is hierarchical clustering<sup>13</sup> based on the idea that nodes belonging to the same community share similar characteristics, which can be quantitatively determined through some properly defined similarity measure. Another approach is the generative model based statistical inference methods.<sup>14–23</sup> It can also occur that a subset of nodes can appear in different communities, which is particularly common in social networks where an individual can appear in different friendship or social groups, leading to overlapping communities. The method based on cliques, subnetworks in which all nodes are

fully connected with all other nodes, can be used to detect communities and to find the hidden overlapping community structure.<sup>24–26</sup> The fundamental issue of the detectability of the community structure has also been addressed.<sup>27–30</sup> The principle and methodology of community detection have one particularly important application in network science: finding missing links and identifying false links from data.<sup>31,32</sup>

In this paper, we propose a novel, “game-change” type principle to address the network community detection problem. Differing drastically from the previous approaches that broadly treat community detection as a structural optimization problem, we ask whether the modular structure of a network can “come out” naturally or emerge automatically as a consequence of the nonlinear dynamical evolution of the system. More specifically, given a network, we assume certain nodal dynamical processes and regard the whole network as a system of coupled nonlinear elements that evolve continuously with time. Generically, a coupled nonlinear dynamical network can exhibit a rich variety of collective dynamics, and our goal is to identify one that naturally reveals the hierarchical community structure of the network. For this purpose, it is necessary to have a control parameter, the tuning of which can lead to distinct dynamical states of the network. The scenario that we seek to establish is that, as the control parameter is tuned systematically, the system would exhibit distinct collective dynamics on different scales, thereby “automatically” revealing the hierarchical organization of the network into communities at distinct scales. For a coupled networked system, a natural choice of the control parameter is the coupling strength between any nodal pair. The advantage of this dynamical approach to community detection lies in the ease with computational implementation: for a given network, one simply implements certain dynamical processes and monitors the collective dynamics as the control parameter is varied and, for some optimal value of the parameter, the community structure would manifest itself naturally and unambiguously in the collective dynamical state of the system.

A candidate of collective dynamics that can naturally reveal the community structure is synchronization, a phenomenon that has been studied extensively in the complex network literature.<sup>33–48</sup> There were previous works demonstrating that synchronization can reveal the topological scales in complex networks.<sup>49–54</sup> Of particular relevance to our work are the studies of synchronization in complex modular networks<sup>44–48</sup> and the phenomenon of clustered synchronization.<sup>55–62</sup> For example, studies on the effects of the modular structure on network synchronizability revealed that a significant imbalance between the intra-modular and inter-modular links can be detrimental to synchronization,<sup>44,45</sup> and network symmetries play a fundamental role in the emergence of clustered synchronization.<sup>57</sup> In spite of the vast literatures on network synchronization, to our knowledge, there has been no previous work on exploiting the emergence and evolution of clustered synchronization for detecting the *hierarchical* community structure.

The main accomplishments of this paper are described as follows: Given a network, we impose an identical chaotic dynamical process on each node, and so, a global synchronization manifold is well defined. As the coupling parameter is

reduced from the global synchronization regime, the system evolves into distinguishable states of clustered synchronization. Unlike global synchronization in which all eigenmodes must be stable with respect to perturbations transverse to the synchronization manifold, in a state of clustered synchronization, there are unstable eigenmodes. In this case, the state vector of the system is dominantly characterized by the linear combination of the eigenvectors associated with the divergent eigenmodes. We argue that these eigenmodes reflect the partition of the network into communities and, as the number of unstable eigenmodes is increased, the community structure at increasingly smaller scales emerges. Using synthetic and real networks, we demonstrate that their hierarchical community structures can be gradually but efficiently unfolded through clustered synchronization. By tuning the coupling parameter to control the number of divergent eigenmodes, we can accurately modulate the degree of synchronization to identify the communities belonging to different hierarchies of the network through the emergent clusters of locally synchronized nodes. Computationally, evolving the underlying coupled networked dynamical system and identifying the various clusters of local synchronization as the coupling parameter is varied adiabatically (i.e., the rate of change of the parameter should be much smaller than the rate of change of a typical dynamical variable of the system), the community structure of the network can be automatically revealed. Comparing with the previous, structure manipulation based methods on community detection, our dynamical evolution based approach is computationally efficient and can readily scale to large networks, completely overcoming the difficulty of NP-hardness.

## II. THEORETICAL METHODS

The collective dynamics of a network of coupled nonlinear oscillators are determined by (1) the network structure as characterized by the Laplacian matrix  $L$  and (2) the nodal dynamical system. For synchronous dynamics, the standard theoretical framework is the master stability function (MSF).<sup>63,64</sup> Briefly, the MSF is the largest transverse Lyapunov exponent that controls the stability of the global synchronization state (manifold) with respect to perturbations transverse to the manifold. In general, the MSF depends on the form of the nodal dynamical system and a generalized coupling parameter  $\varepsilon$ . If there exists an interval of  $\varepsilon$  in which the MSF is negative, global synchronization can occur in this parameter interval. The generalized coupling parameter  $\varepsilon$  is related to the original coupling parameter  $\sigma$  of the network through the eigenvalues of its Laplacian matrix:  $\varepsilon = \sigma\lambda$ . If the network size is  $N$ , there are  $N$  distinct eigenvalues of the Laplacian matrix (including the trivial one):  $0 = \lambda_1 < \lambda_2 \dots < \lambda_N$ . For the network system,  $\varepsilon$  can then take on  $(N-1)$  nontrivial values:  $\sigma\lambda_2, \dots, \sigma\lambda_N$ . Only when all these  $(N-1)$  values fall within the interval in which the MSF is negative, global synchronization is stable and physically realizable. As the value of the original coupling parameter is decreased, the discrete set of  $\varepsilon$  values begin to move out of the stable synchronization interval through its lower bound (towards left), making the  $(N-1)$  transverse

subspaces corresponding to the eigenmodes lose stability one after another and inducing desynchronization. The existence of a finite lower bound of the stable synchronization interval is thus key to our community detection method. A previous work demonstrated that such a lower bound indeed exists for typical nonlinear oscillators.<sup>64</sup> Because of the flexibility in the nodal dynamical system for community detection, we choose the ones where the lower bound is finite and not arbitrarily close to zero, such as the classic chaotic Rössler<sup>65</sup> and Lorenz<sup>66</sup> oscillators.

For an undirected network of  $N$  coupled chaotic oscillators, the Laplacian matrix is given by  $L = D - A$ , where  $A$  is the network adjacency matrix and  $D$  is a diagonal matrix of degree ( $\text{diag}(k_1, k_2, \dots, k_N)$ ). Let  $\{\mathbf{v}_1, \mathbf{v}_2, \dots, \mathbf{v}_N\}$  be the set of eigenvectors associated with the set of  $N$  eigenvalues:  $0 = \lambda_1 < \lambda_2 < \dots < \lambda_N$ . Each individual oscillator's dynamics can be described by an  $n$ -dimensional state vector  $\mathbf{x}_i$  ( $\mathbf{x}_i = [x_{i,1}, x_{i,2}, \dots, x_{i,n}]^T$ ) governed by the equation  $\dot{\mathbf{x}}_i = \mathbf{F}(\mathbf{x}_i)$ . The dynamics of the network of  $N$  such coupled oscillators are governed by

$$\dot{\mathbf{x}}_i = \mathbf{F}(\mathbf{x}_i) - \sigma \sum_{j=1}^N l_{ij} \mathbf{H}(\mathbf{x}_j), \quad \text{for } i = 1, \dots, N, \quad (1)$$

where  $l_{ij}$  denote the elements of  $L$  and  $\mathbf{H}(\mathbf{x}_j)$  is the coupling function. Due to the constraint of the elements of the Laplacian matrix:  $\sum_{j=1}^N l_{ij} = 0$ , a global synchronization state  $\mathbf{s}$  exists for  $t \rightarrow \infty$ :  $\mathbf{x}_1 = \mathbf{x}_2 = \dots = \mathbf{x}_N \equiv \mathbf{s}$ . Let  $\delta\mathbf{x}_i = \mathbf{x}_i - \mathbf{s}$  be a small variation in the  $i$ th oscillator's state from the synchronization manifold. We have

$$\delta\dot{\mathbf{x}}_i = D\mathbf{F}(\mathbf{s}) \cdot \delta\mathbf{x}_i - \sigma D\mathbf{H}(\mathbf{s}) \cdot \sum_{j=1}^N l_{ij} \delta\mathbf{x}_j, \quad \text{for } i = 1, \dots, N. \quad (2)$$

Letting  $\delta\mathbf{x} \equiv [\delta\mathbf{x}_1, \delta\mathbf{x}_2, \dots, \delta\mathbf{x}_N]$ , we can rewrite Eq. (2) as

$$\delta\dot{\mathbf{x}} = D\mathbf{F}(\mathbf{s}) \cdot \delta\mathbf{x} - \sigma D\mathbf{H}(\mathbf{s}) \cdot \delta\mathbf{x} \cdot L^T. \quad (3)$$

To diagonalize Eq. (3), we set the variations as the linear combination of the eigenvectors of  $L$ :  $\delta\mathbf{x}^T = \mathbf{O} \cdot \boldsymbol{\xi}^T$ , where  $\boldsymbol{\xi} = [\xi_1, \xi_2, \dots, \xi_N]$  are the coefficients of the linear combination and  $\mathbf{O}$  is the eigenvector matrix. We have

$$\dot{\boldsymbol{\xi}} = D\mathbf{F}(\mathbf{s}) \cdot \boldsymbol{\xi} - \sigma D\mathbf{H}(\mathbf{s}) \cdot \boldsymbol{\xi} \cdot \Lambda, \quad (4)$$

where  $\Lambda \equiv \text{diag}(\lambda_1, \lambda_2, \dots, \lambda_N)$ . Since  $\lambda_1 = 0$ , the equation  $\dot{\boldsymbol{\xi}} = D\mathbf{F}(\mathbf{s}) \cdot \boldsymbol{\xi}$  describes the dynamics within the synchronization manifold. The remaining  $(N-1)$  eigenmodes are decoupled, which are governed by

$$\dot{\xi}_i = [D\mathbf{F}(\mathbf{s}) - \sigma\lambda_i D\mathbf{H}(\mathbf{s})] \cdot \xi_i, \quad \text{for } i = 2, 3, \dots, N. \quad (5)$$

The  $(N-1)$  equations in Eq. (5) determine the transverse stabilities of the  $N-1$  eigenmodes, with MSF being the maximum Lyapunov exponent associated with Eq. (5).

The eigenvalues and the associated eigenvectors of the Laplacian matrix are closely related to the hierarchical community structure of the network.<sup>49,67</sup> Near the global

synchronization regime, the values of the elements of  $\mathbf{v}_2$  associated with oscillators in the same community are similar,<sup>68</sup> leading to the emergence of clustering of oscillators. When the network contains two distinct communities only, the eigenvector  $\mathbf{v}_2$  can be used as a criterion for detecting the communities. For a hierarchical network with  $m$  ( $\geq 2$ ) communities, the first  $m-1$  non-trivial eigenvalues of the Laplacian matrix are much smaller than the rest, forming a gap between  $\lambda_m$  and  $\lambda_{m+1}$ , as shown in Fig. 1. In general, information about the partition of the communities in multi-level hierarchies is encoded in the eigenvectors.

To make the eigenmodes corresponding to the first  $m$  eigenvalues transversely unstable while keeping the rest stable, we can modulate the coupling parameter as

$$\sigma_m = \frac{1}{2} \left[ \frac{\varepsilon_1}{\lambda_m} + \frac{\varepsilon_1}{\lambda_{m+1}} \right], \quad m = 2, 3, \dots, N-1, \quad (6)$$

where  $\varepsilon_1$  denotes the lower boundary of the global synchronization region in terms of the generalized coupling parameter. To guarantee that the remaining  $(N-m)$  eigenmodes are transversely stable, we impose the following restriction on the coupling parameter:

$$\sigma_m \lambda_N \leq \varepsilon_2, \quad m = 2, 3, \dots, N-1, \quad (7)$$

where  $\varepsilon_2$  is the upper boundary of the global synchronization region. For a variety of classic nonlinear oscillators, it is common to have<sup>64</sup>  $\varepsilon_2 = \infty$ , and so, Eq. (7) would hold trivially.

We preserve the eigenvectors associated with the first  $m$  eigenvalues, which contain information about the community division. Since the variation of an individual oscillator is a linear combination of the eigenvectors, its elements of the state vector are correlated with the eigenvectors. When

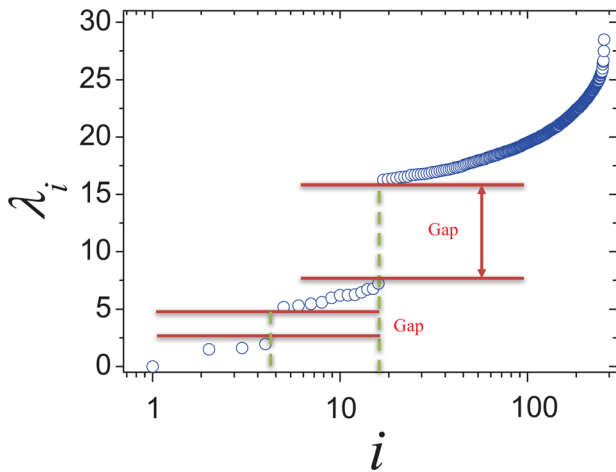


FIG. 1. Spectral characteristics of a benchmark network with two hierarchical levels of communities. The network has  $N=256$  nodes equally distributed among 16 communities that constitute the first hierarchical level, which belong to four larger communities at the second level, each containing four smaller communities at the first level. For each node, the numbers of edges within the first and second levels are 14 and 3, respectively, henceforth the notation (14, 3) to name the network. Shown are the eigenvalues of the Laplacian matrix in an ascending order:  $0 = \lambda_1 < \lambda_2 \dots < \lambda_{256}$ . There exist two gaps in the eigenvalue ordering: one between  $\lambda_4$  and  $\lambda_5$  and the other between  $\lambda_{16}$  and  $\lambda_{17}$ , corresponding to the two hierarchies in the community structure of the network.

the system evolves towards clustered synchronization, the trajectories of the oscillators in the same communities approach each other, but those of the oscillators belonging to different communities diverge. The community structure of the network can then be faithfully detected by monitoring the clustering behavior of oscillators through their state vectors. As we have demonstrated, even the hierarchical community structure can be revealed by controlling the coupling parameter with respect to the occurrence of clustered synchronization at different levels.

### III. RESULTS

We demonstrate the effectiveness of our nonlinear dynamical evolution based approach to detecting hierarchical communities by using a class of synthetic, benchmark networks with the flexibility of generating a wide spectrum of community structures,<sup>49</sup> as well as a number of empirical networks.

#### A. Benchmark hierarchical community network

We use the synthesized network model<sup>49</sup> that has been the standard tested in the field. A benchmark network consists of 16 non-overlapping communities and 256 nodes in total, which are uniformly distributed among the communities. The 16 communities represent the first hierarchical level, which are uniformly aggregated into four non-overlapping, larger communities that constitute the second hierarchical level. Some key structural information of the individual communities at two levels is listed in Tables I and II, respectively. For each node, the numbers of edges at the first and second levels are denoted as  $z_1$  and  $z_2$ , respectively, while the number of edges within its own smallest community is  $z_{in}$ . The edge numbers are constrained by the relation  $z_1 + z_2 + z_{in} = 18$ . Different choices of the values of  $(z_1, z_2)$  lead to networks with varying modularity. For convenience, we use the notation  $(z_1, z_2)$  to denote a particular modular network. For example, the modularity associated with the first hierarchical

TABLE I. Average degree  $\langle k \rangle$  and clustering coefficient  $C$  of each community at the first hierarchical level for the benchmark system.

Community	$\langle k \rangle$	$C$
1	13.75	0.907
2	13.75	0.907
3	13.75	0.906
4	13.88	0.915
5	13.75	0.907
6	13.88	0.915
7	13.75	0.906
8	13.88	0.916
9	13.88	0.915
10	13.88	0.915
11	13.62	0.898
12	13.88	0.916
13	13.62	0.900
14	14.00	0.923
15	13.62	0.900
16	13.88	0.915



TABLE II. Average degree  $\langle k \rangle$  and clustering coefficient  $C$  of each community at the second hierarchical level for the benchmark system.

Community	$\langle k \rangle$	$C$
1	16.59	0.641
2	16.78	0.631
3	16.72	0.637
4	16.75	0.634

level can be adjusted by varying  $z_1$  and  $z_2$ , which ranges approximately from the value of 0.77 [(15, 2) network] to 0.54 [(11, 6) network]. Because of the constraint in the edge numbers, for the networks with different modularity values at the first level, their modularity associated with the second hierarchical level assumes the identical value of 0.66. As a concrete example to gain insight into the underlying mechanism of our dynamical evolution based community detection framework, we consider a (14,3) network. Figure 1 shows the eigenvalues of the Laplacian matrix  $L$  in an ascending order, where it can be seen that the first 16 eigenvalues are much smaller than the rest, with a distinct gap between the two groups, indicating the emergence of 16 communities at the first hierarchical level. Another distinct gap exists between the fourth and fifth eigenvalues, suggesting the existence of four larger communities at the second hierarchical level.

We demonstrate that the hierarchical community structure can manifest itself as synchronized clusters in the dynamical evolution of the system. Given a network of known topology, we impose a nonlinear dynamical process that is identical for all nodes and decrease the coupling parameter from the regime of global synchronization, in which all nodes exhibit completely identical dynamical evolution. Convenient choices of the nodal dynamics are the classic chaotic Rössler<sup>65</sup> and Lorenz<sup>66</sup> oscillators, with both being three-dimensional, where the former is defined by the velocity field  $\mathbf{F} = [-(y+z), x+0.2y, 0.2+z(x-9)]^T$  and the latter is described by  $\mathbf{F} = [10(y-x), x(28-z)-y, xy-(8/3)z]^T$ . We assume a simple linear coupling scheme in which the node-to-node interactions occur only through the first component of the nodal dynamical variable, i.e., the coupling vector is  $\mathbf{H}(\mathbf{x}) = [x, 0, 0]^T$ .

We carry out a synchronization analysis for the (14,3) network, whose eigenvalue spectrum is displayed in Fig. 1. For nodal dynamics of the chaotic Rössler type, the synchronization region is  $[\varepsilon_1, \varepsilon_2] = [0.2, 5]$ , where  $\varepsilon = \sigma\lambda$  is a generalized coupling parameter ( $\sigma$  is the original coupling parameter and  $\lambda$  denotes an eigenvalue “variable” that takes on the specific eigenvalues of the Laplacian matrix, which are ordered as  $0 = \lambda_1 < \lambda_2 \dots < \lambda_N$ ). To present results in correspondence to the eigenvalue spectrum in Fig. 1, we specify the coupling parameter  $\sigma$  in terms of an integer parameter  $m$ , where for any specific value of  $m$ , the first  $m-1$  nontrivial eigenmodes, i.e., from  $\lambda_2$  to  $\lambda_m$ , of the Laplacian matrix are unstable with respect to perturbations transverse to the synchronization manifold, while the remaining  $(N-m)$  eigenmodes are stable. In the parameter region of interest, global synchronization is thus not possible. For certain specific values of  $m$ , e.g.,  $m=4$  and  $m=16$ , the networked system exhibits distinct clusters of synchronous nodes.

To characterize clustered synchronization more accurately, we define the following order parameter for a given value of  $m$ :

$$r_L(m) = \frac{(1/N) \sum_{i=1}^N \sqrt{(x_i - \bar{x})^2 + (y_i - \bar{y})^2 + (z_i - \bar{z})^2}}{(1/M) \sum_{(i,j) \in E} \sqrt{(x_i - x_j)^2 + (y_i - y_j)^2 + (z_i - z_j)^2}}, \quad (8)$$

where  $N$  and  $M$  are the number of nodes and the number of synchronous clusters, respectively. According to Eq. (6), the quantity  $m$  affects the value of  $\sigma_m$ , which indirectly determines the value of  $r_L(m)$  through synchronization. In Eq. (8), the numerator measures the extent of global synchronization, while the denominator quantifies the degree of clustered synchronization. Note that for a given community network, the ratio  $\frac{M}{N}$  is independent of  $m$  and affects the values of  $r_L(m)$  equally for different values of  $m$ . The value of  $M$  can be estimated using the optimal synchronization error matrices. Figure 2 shows the absolute difference  $|r_L(m+1) - r_L(m)|$  as a function of  $m$  for  $m = 1, \dots, N-1$ . There are two peaks: one at  $m=4$  and the other at  $m=16$ , indicating that for the (14,3) network, simultaneous optimization of clustered synchronization and community partition occurs at two hierarchical levels. (More examples are provided in Appendix A.)

To visualize clustered synchronization, we use the pairwise Euclidean distance between the state vectors of any nodal pair, which is the synchronization error. We first test the Rössler nodal dynamics with the initial values of the dynamical variables chosen randomly from the interval  $[0, 1]$ . The evolution time is set (rather arbitrarily) to  $T=100$ , which contains approximately two dozen of oscillating cycles of the chaotic Rössler oscillator. For each value of the coupling parameter, we construct an  $N \times N$  synchronization error

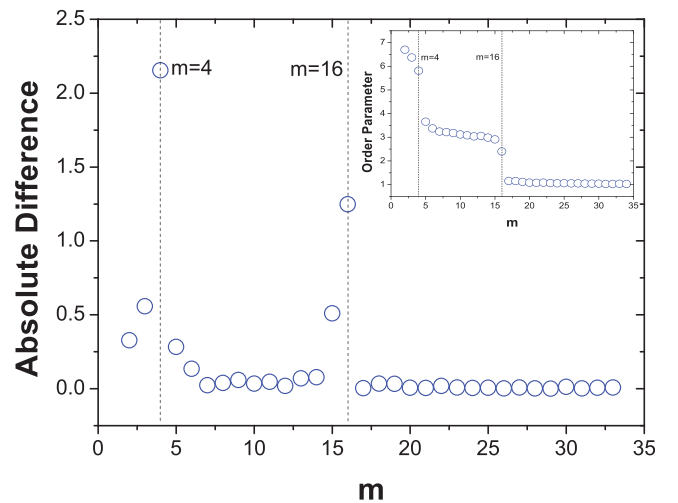


FIG. 2. Absolute differences in the order parameter values as a function of  $m$ . For the (14,3) network, the order parameter versus  $m$  exhibits two peaks: one at  $m=4$  and the other at  $m=16$ , signifying optimal clustered synchronization and community partition at the two corresponding hierarchical levels. The inset shows changes in the order parameters as a function of  $m$ .

matrix for all possible nodal pairs, averaging over 100 statistical realizations of the dynamical trajectory. Figure 3 shows, for 18 different values of the coupling parameter as represented by  $m$ , the pairwise synchronization error matrices, where the error values are distinguished by different colors. It is striking that as the value of  $m$  is increased from two to 19, synchronized clusters with a hierarchical community structure are gradually unfolded by the matrix representation. For the values of the coupling strength corresponding to  $m=4$  and  $m=16$ , both the number and the size of synchronous clusters are in complete agreement with the community structures of the network at the two levels. Particularly, for  $m \leq 4$ , there are four synchronous clusters that correspond exactly to the four large communities at the second hierarchical level, due to the transversely unstable eigenmodes associated with  $\lambda_2$ ,  $\lambda_3$ , and  $\lambda_4$ . In this case, there is no synchronization over the scale of this modular hierarchy, making it possible to discern the communities at the corresponding scale. Equivalently, the community structure at this scale is encoded faithfully in the eigenvectors associated with these eigenmodes. However, at a smaller scale, the nodal dynamics are synchronized, due to the transverse stability of the vast majority of eigenmodes. As the value of  $m$  is increased from 4 to 16, starting from  $m=5$ , the eigenmodes lose transverse stability sequentially, leading to a gradual deterioration of the original synchrony within each larger community. That is, the corresponding eigenvectors begin to reveal the community structure at a smaller scale. For  $m=16$ , all 15 nontrivial eigenmodes (from  $m=2$  to  $m=16$ ) have become unstable, and the smaller modular structure at the first hierarchy of 16 communities emerges unambiguously. For  $m \geq 17$ , additional eigenmodes become

transversely unstable, revealing more detailed and refined structures within each of the 16 communities.

To better visualize the emergence of local synchronous clusters as a result of the hierarchical community structure of the network, we generate polar dendrogram plots of the agglomerative hierarchical trees for  $m=4$ , 16, and 19, as shown in Fig. 4(a). A dendrogram is a tree diagram to illustrate and distinguish the clusters with a hierarchical structure based on certain distance metrics. In our case, the Euclidean synchronization error is a natural choice of the distance metric, and the clusters are drawn based on the values of the error. As shown in Fig. 4(a), for  $m=4$ , four distinct clusters at the second hierarchical level exist, where the synchronization errors within any single cluster are significantly smaller than the inter-cluster errors. For  $m=16$ , clusters in the first hierarchy can be distinguished, as shown in Fig. 4(b), where the existence of two hierarchies can be ascertained. In fact, this is the optimal value of  $m$  for which the hierarchical community structure can be best unraveled and visualized. For  $m=19$ , the hierarchical structure (especially those at the first level) begins to deteriorate, as the synchronization state is restricted to within some (not all) communities at the first hierarchical level, as shown in Fig. 4(c), where some of the 16 small synchronous clusters appear to be connected. These results thus demonstrate, in a visually intuitive manner, how the network dynamical state evolves to reveal the hierarchical community based on local or clustered synchronization. In the particular case of coupled chaotic Rössler oscillators, global synchronization occurs in a finite interval of the generalized coupling parameter.<sup>63,64</sup> As  $m$  is increased from one, the values of the generalized coupling parameter

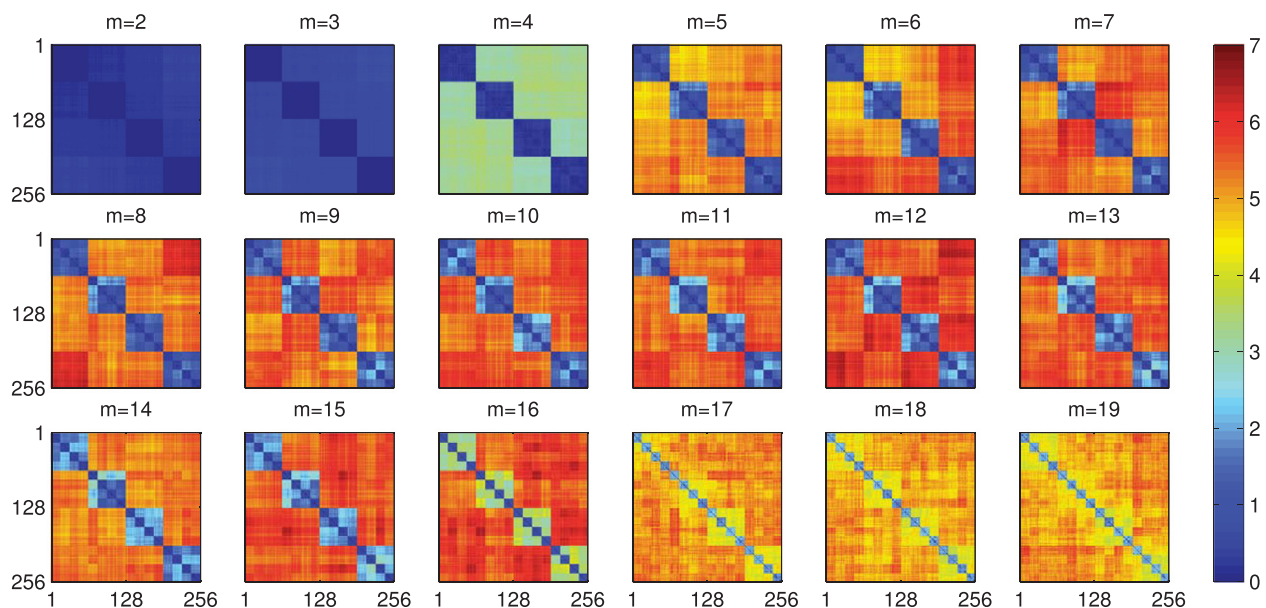


FIG. 3. Emergence of the hierarchical community structure through synchronization. The benchmark network has the structure of (14,3), with its eigenvalue spectrum shown in Fig. 1. The nodal dynamical system is that of a chaotic Rössler oscillator. The coupling parameter is continuously decreased so that, starting from  $m=2$ , the nontrivial eigenmodes lose their transverse stability one after another. Shown is the synchronization error matrix constructed from all the pairwise distances between the nodal dynamical variables, where the distances are color coded. For each panel, the integer value of  $m$  corresponds to the case where the  $(m-1)$  nontrivial eigenmodes (from two to  $m$ ) are transversely unstable. For  $m \leq 4$ , the synchronization states reflect correctly the four large communities at the second hierarchical level. As  $m$  is increased from 4 to 16 (corresponding to the continuous decrease in the actual value of the coupling parameter), the degree of inter-community synchronization at the first hierarchical level of 16 communities is gradually weakened, revealing the community structure at the smaller scale. Insofar as  $m \leq 16$ , there is local synchronization within each of the 16 communities. For  $m \geq 17$ , synchronization at the small scale begins to deteriorate, revealing more refined structures within each such community.

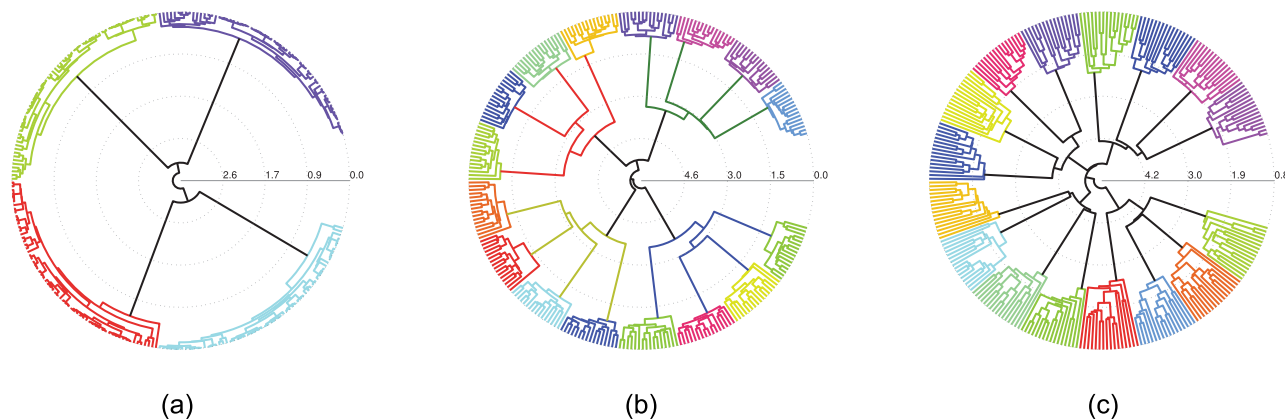


FIG. 4. Polar dendrograms of synchronous clusters reflecting the hierarchical community structure of the network. (a)–(c) Polar dendrograms generated from synchronization errors as the distance metric for  $m = 4, 16,$  and  $19,$  respectively. For  $m = 4,$  the dendrogram reveals 4 large communities. For  $m = 16,$  the two-level hierarchy and 16 smaller communities are unfolded. For  $m = 19,$  the hierarchical community structure with the 16 small communities becomes deteriorated. (a)  $m = 4,$  (b)  $m = 16,$  and (c)  $m = 19.$

associated with the eigenmodes move out of the interval through the left (lower) boundary one after another, rendering unstable global synchronization but leading to the emergence of clustered synchronization which, for a proper value of  $m,$  can reveal the intrinsic hierarchical community structure of the network.

The emergence of clustered synchronization and its power in revealing the underlying hierarchical community structure of the network do not depend on the specific nodal dynamical system, insofar it generates nonlinear oscillatory behaviors with a finite lower bound of the interval in the generalized coupling parameter in which all nontrivial eigenmodes are transversely stable so that the whole network is globally synchronizable.<sup>63,64</sup> In this case, “pushing” the generalized coupling parameter associated with the originally transversely stable eigenmodes out of the interval through the lower bound leads to desynchronization at the global scale but to optimal clustered synchronization reflecting accurately the community structure. To test the generality and robustness of this principle, we perform computations using a different oscillator system, the classic chaotic Lorenz system,<sup>66</sup> and choose the original coupling parameter  $\sigma$  in a somewhat arbitrary manner. Figure 5 shows, for the benchmark network (14, 3), the synchronization error matrices for  $\sigma = 4, 3, 2$  and  $1,$  respectively. We obtain essentially the same results as for the Rössler oscillator (Fig. 3): as the coupling parameter is decreased, global synchronization is replaced by clustered synchronization reflecting accurately the hierarchical community structure.

**B. Real networks**

We test our synchronization based approach to community detection on a number of real world networks and present results for two of them: the American college football game network (CFGN)<sup>1</sup> and the southern women club network (SWCN)<sup>69</sup> (more examples are given in Appendix B). The CFGN consists of 115 teams (nodes), which are uniformly divided into 12 conferences (communities at the small scale) and form the hierarchical community structure through games, as shown in Fig. 6. The key structural information

about the individual communities of CFGN is listed in Table III. The nodal dynamics are set to be the chaotic Rössler type. A systematic reduction in the value of the coupling parameter is represented by a change in  $m$  (the number of nontrivial, transversely unstable eigenmodes) from 2 to 13. The evolution time is  $T = 30.$  The synchronization error matrices for these values of  $m$  are shown in Fig. 7. For  $m \leq 7,$  synchronous clusters consisting of several conferences arise, indicating a high hierarchical level of the community structure. As the value of  $m$  is increased from 8 to 13, synchronization among the conferences is weakened. As a result, the synchronous clusters are restricted to the first hierarchical level, i.e., the conference level. Because of the insufficient number of games played within the “Independent” and “Sun Belt”

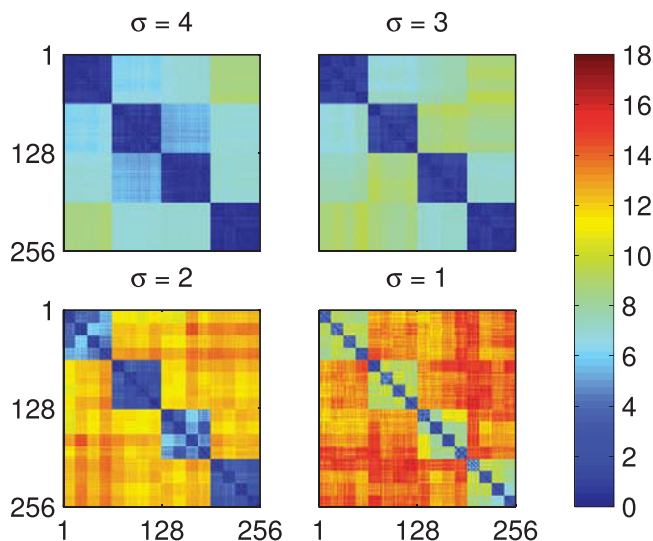


FIG. 5. Uncovering the hierarchical community structure via clustered synchronization with the nodal dynamical system being the classic chaotic Lorenz oscillator. For the benchmark network (14, 3), synchronization error matrices for values of the original coupling parameter  $\sigma = 4, 3, 2,$  and  $1,$  respectively. The simulation time is  $T = 100,$  which contains about a few tens of cycles of oscillation. A decrease in the value  $\sigma$  results in a transition in the network dynamics from global to clustered synchronization, revealing the two-level hierarchical community structure of the network.



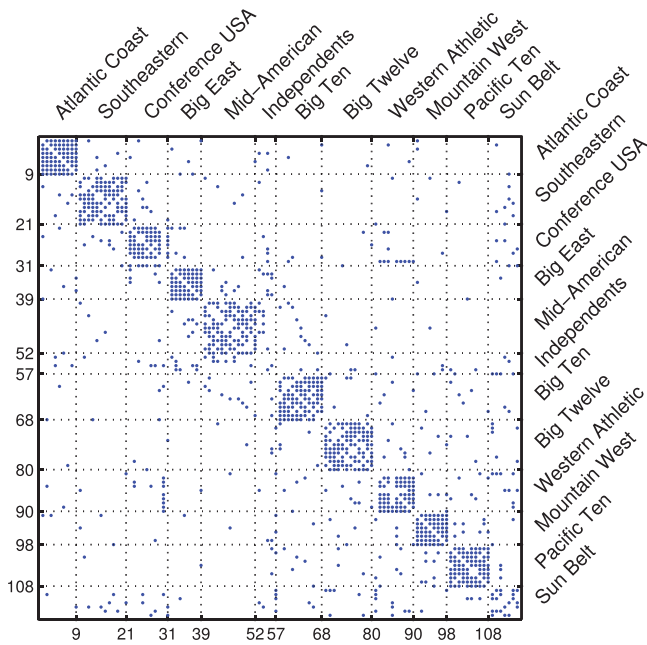


FIG. 6. Structure of the American college football game network as represented by the adjacency matrix. There are altogether 115 teams (115 nodes in the network), which are divided into 12 conferences—separated by lines. The names of the conferences are noted. Intra-conference games are more frequent than the inter-conference ones, giving rise to a community structure. Two anomalies are the “Independents” and “Sun Belt” conferences, which have fewer intra-conference games. The conferences are organized into a hierarchical structure because inter-conference teams that are geographically close to one another are more likely to play in a game.

conferences, the corresponding synchronous clusters are largely absent. The polar dendrogram representations of the synchronous clusters (and hence the hierarchical community structure) as the agglomerative hierarchical trees for three values of  $m$  (2, 7, and 12) are shown in Fig. 8, from which 2, 7, and 10 major clusters can be seen. More specifically, as shown in Fig. 8(a), the CFGN is divided into two equivalent communities, corresponding to teams from the east and west areas, which constitute the highest hierarchical level. The two large communities approximately split into four communities, each corresponding to a single conference and other three

TABLE III. Average degree  $\langle k \rangle$  and clustering coefficient  $C$  of the 12 conferences in the American football game network.

Community	$\langle k \rangle$	$C$
Atlantic Coast	8.0	1.00
Big East	7.0	1.00
Big Ten	8.0	0.75
Big Twelve	8.0	0.68
Conference USA	6.2	0.74
Independents	0.4	0.00
Mid-American	7.7	0.64
Mountain West	7.0	1.00
Pacific Ten	8.0	0.86
Southeastern	8.0	0.68
Sun Belt	2.9	0.83
Western athletic	6.0	0.86

made up of conferences whose teams are geographically close. Finally, the small communities associated with the conferences can be detected reliably by partitioning the hierarchical tree into 10 major clusters, as shown in Fig. 8(c). Note that teams in the same conferences form communities at the first hierarchical level and geographically close conferences form larger scale communities at higher hierarchical levels. There is thus a good agreement between the hierarchical structures unfolded by clustered synchronization and the organizing principle of the games.

Our second real-world example is an empirical bipartite network, the southern women club network.<sup>69</sup> The network contains 18 women and 14 social events, and an edge exists between a woman and an event if she attended the event, as shown in Fig. 9(a). In an early work,<sup>69</sup> general ethnographic knowledge was used to assign the women to two groups, consisting of women 1–9 and 10–18, respectively. For the purpose of further demonstration of the generality with respect to variations in the setting of the dynamical system, we choose a slightly different parameter combination for the chaotic Rössler oscillator from that in Fig. 1, which is described by  $\mathbf{F} = [-(y+z), x+0.2y, 0.2+z(x-12)]^T$ , as well as a different coupling function:  $\mathbf{H}(\mathbf{x}) = [x, y, z]^T$ . For these nodal dynamics and coupling settings, with respect to the generalized coupling parameter, global synchronization occurs in the region  $[0.1, \infty]$ . We choose the coupling strength corresponding to  $m=2$ , as only two synchronizing clusters are expected according to priori knowledge. The synchronization error matrix is shown in Fig. 9(b), where either the women or the event groups constitute two major synchronous clusters as indicated by the diagonal blocks of the matrix. Specifically, for the women group, the individuals 1–9 and 10–16 form two communities, but the individuals 17 and 18 are not included because they both were associated with only two events. To better visualize clustered synchronization, we adjust the nodal order in Fig. 9(c), where the two major synchronous clusters including nodes from two parts of the bipartite network are more distinct. We also note, as in the early work,<sup>69</sup> that the communities consisting of nodes from both sides reflect the preferences of women from different social groups.

#### IV. CONCLUSION AND DISCUSSION

In the past two decades, there has been tremendous development in the investigation of the interplay between complex network structures and dynamics. A well-studied subject is how the network structure affects the collective dynamics. There have been relatively few studies in the opposite direction, i.e., on the problem of how dynamics may be exploited to understand and reveal the network structure. Community detection is essentially a problem of network structure analysis and manipulation. It is known as one of the most difficult problems in network science because of its NP-hard nature. Aiming to develop a drastically different approach from those based on structure exploration in existing works, we seek to uncover hierarchical community structures through the evolution of collective dynamics. The new twist in our work is that, with a choice of the collective

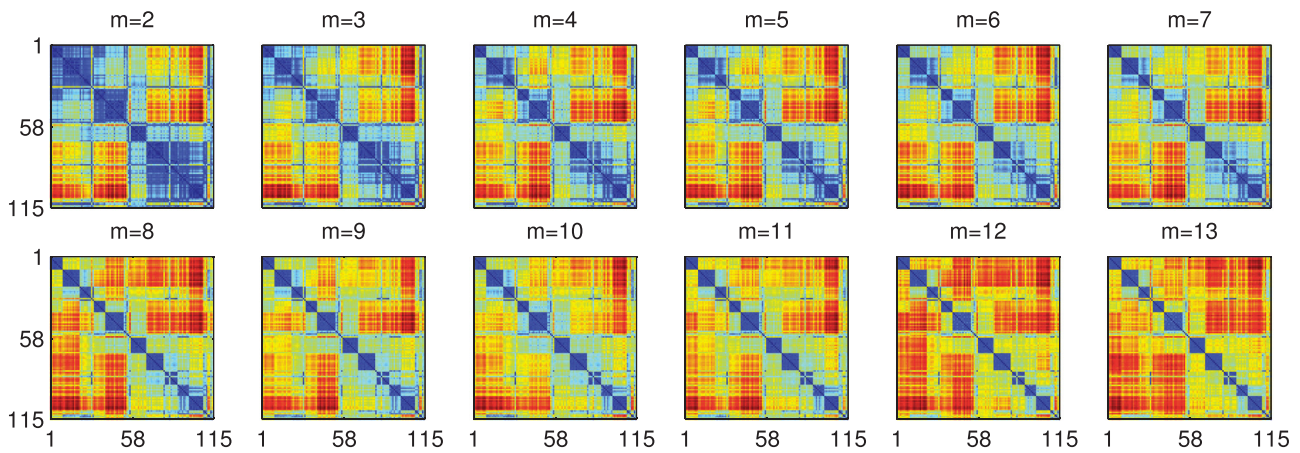


FIG. 7. Detection of the community structure of the American college football game network through clustered synchronization. Shown are the synchronization error matrices for the American football game network with the value of  $m$  ranging from 2 to 13. Nodes are plotted in the same order as in Fig. 6. As a result, the conferences (communities) are placed in the same sequence as in the matrices. The matrices are scaled into different color maps for clear visualization, where the blue and red colors indicate small and large synchronization errors, respectively. For  $m \leq 5$ , synchronous clusters consisting of several conferences are apparent. As  $m$  is increased from 6 to 13, the degree of synchronization between different conferences weakens. There is a unique correspondence between a conference and a synchronous cluster for most conferences (except two). The two exceptions are the “Independent” and “Sun Belt” conferences due to the insufficient number of games played within each of them.

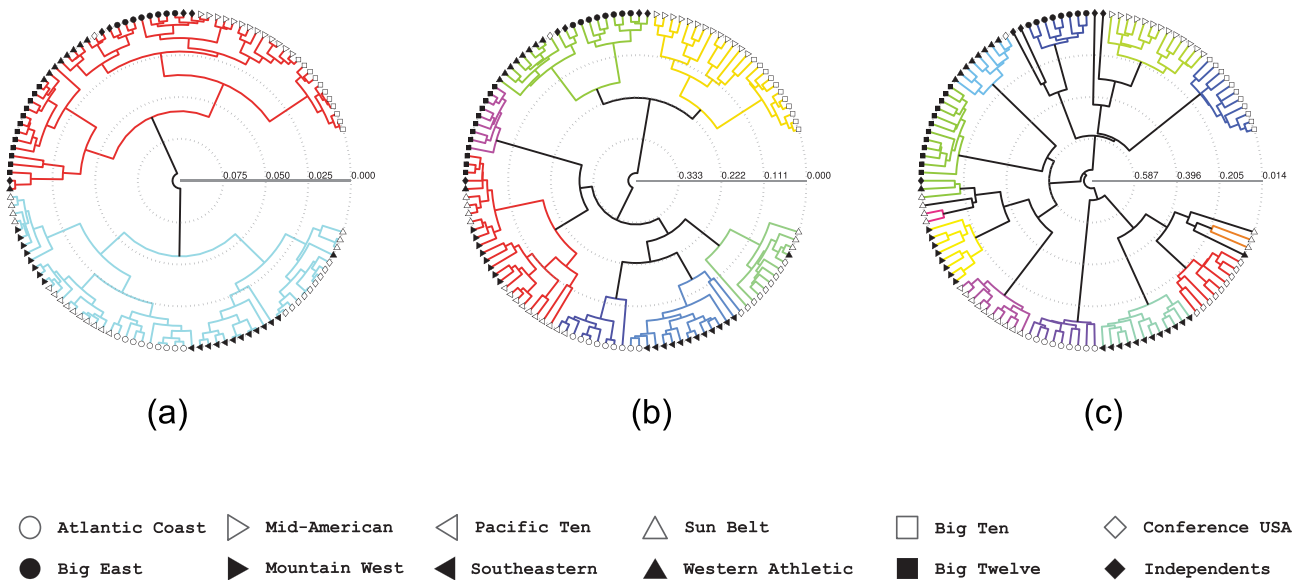


FIG. 8. Polar dendrograms of synchronous clusters for the community structure of the American college football game network. (a)–(c) Agglomerative hierarchical trees for  $m=2, 7$ , and  $12$ , respectively. The cluster trees are partitioned into 2, 7, and 10 major clusters in (a), (b), and (c), respectively. Different markers of nodes indicate the conferences to which the nodes belong. Teams in the same conferences form communities at the first hierarchical level, and geographically close conferences form large scale communities at higher hierarchical levels. The hierarchical structures unfolded by clustered synchronization reflect accurately the organizing principle of the games. (a)  $m = 2$ , (b)  $m = 7$ , and (c)  $m = 12$ .

dynamics and under a suitable setting, the dynamical evolution would naturally give out or reveal the structured organization characteristics such as the hierarchical communities. We demonstrate in this paper that this is indeed feasible

through a concrete type of collective dynamics: clustered synchronization.

Implementing nonlinear oscillatory nodal dynamics on the whole network and choosing the value of the coupling

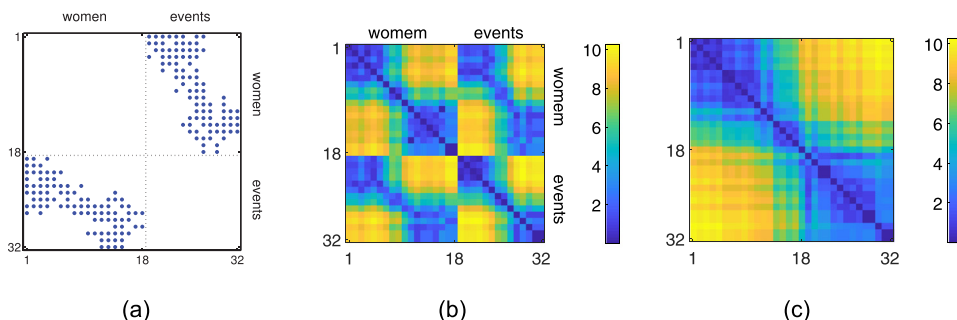


FIG. 9. Synchronization based detection of the community structure of the southern women club network. (a) The network structure as characterized by the adjacency matrix. (b) and (c) Synchronization error matrices in the original and an adjusted nodal order, respectively. The women and event groups are organized into two major synchronous clusters, as indicated by diagonal blocks of nodes.

parameter such that global synchronization is unstable but local or clustered synchronization can occur, we show that an accurate picture of the community structure of the network can be obtained simply through identification of the synchronous clusters. An appealing feature is that, for different choices of the coupling parameter, the synchronous clusters can form at different scales and are organized according precisely to the hierarchical organization of the communities. Imagine that the coupling parameter is controlled by a kind of “knob.” Our main result indicates that, *by turning the knob slowly, the hierarchical community structure at different scales would come out automatically.* More quantitatively, using the standard approach of master stability function, we analyze the emergence of clustered synchronization as the coupling parameter is continuously decreased from the regime of global synchronization. During this process, there is discontinuous breaking of the network synchronization state into clusters of increasingly reduced size, forming synchronous clusters at smaller scales. Distinct subintervals in the coupling parameter arise, in which the synchronous clusters correspond exactly to the community structure at a particular scale. Combining information from all these parameter subintervals reveals accurately the hierarchical community structure of the network. We validate this dynamical evolution based approach using a benchmark network with adjustable intra- and inter-community linkage and test it on a number of real world networks.

We remark that our dynamical evolution based approach to community detection is quite different from the data based network reconstruction problem or reverse engineering of complex networks.<sup>70</sup> For the reconstruction problem, the structure of the network is unknown, and one is to use available data (often time series) to reconstruct the topology<sup>71–74</sup> through a wide variety of approaches from physics, mathematics, and signal processing.<sup>70</sup> In our case, the network topology is given, and we generate a computational model by imposing certain type of dynamical process on the network, with the goal of identifying the community structure at different scales.

Finally, we discuss the potential to exploit clustered synchronization for reconstructing the hidden metric space of complex networks. In particular, we note that the community structure of a network is a coarse representation of the relation among the nodes characterizing whether any two nodes belong to the same community. While the hierarchical organization of communities provides certain topological information about the nodal connection patterns, it does not capture the finer details. For example, clustered synchronization in the American football game network for a certain value of the coupling parameter indicates only that geographically close nodes are more likely to be connected, as shown in Fig. 7, where the geographical distances among the locations of the teams are well correlated with the synchronization degree among the nodes. In this regard, there was a previous work on navigability of complex networks<sup>75</sup> in which a spatial network (e.g., the Internet at the autonomous system (AS) level) is embedded into a hyperbolic hidden metric space with distances proportional to the degree of similarities. In this sense, a wide variety of networks can be

regarded as being generated based on some kind of hidden metric space. We speculate that the degree of synchronization between a pair of nodes is indicative of the distance in the corresponding hidden metric space. If this is indeed the case, then clustered synchronization can be exploited for constructing the hidden metrics space with applications in network navigation, link prediction and recommendation.

## ACKNOWLEDGMENTS

This work was partially supported by the National Natural Science Foundation of China under Grant Nos. 61673086, 11575041, and 61433014, Shandong Provincial Natural Science Foundation, China, under Grant No. ZR2016FQ14, and the Fundamental Research Funds for the Central Universities (Nos. ZYGX2015J153 and ZYGX2016J058). Y.C.L. would like to acknowledge support from the Vannevar Bush Faculty Fellowship program sponsored by the Basic Research Office of the Assistant Secretary of Defense for Research and Engineering and funded by the Office of Naval Research through Grant No. N00014-16-1-2828.

## APPENDIX A: CLUSTERED SYNCHRONIZATION IN SYNTHESIZED BENCHMARK NETWORKS

The synthesized benchmark networks have two hierarchical levels. The 16 communities represent the first hierarchical level, which are uniformly aggregated into four non-overlapping, larger communities that constitute the second hierarchical level. For each node, the numbers of edges at the first and second levels are denoted as  $z_1$  and  $z_2$ , respectively, while the number of edges within its own smallest community is  $z_{in}$ . The edge numbers are constrained by the relation  $z_1 + z_2 + z_{in} = 18$ . The modularity associated with the first hierarchical level can be adjusted by varying  $z_1$  and  $z_2$ , which ranges approximately from the value of 0.77 [(15,2) network] to 0.54 [(11,6) network]. Because of the

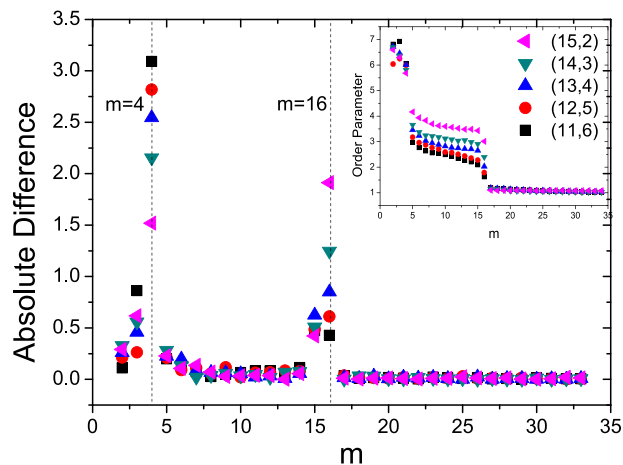


FIG. 10. Absolute differences in the adjacent values of the order parameter as a function of  $m$  for synthesized benchmark networks. Each network possesses two hierarchical levels of modularity, but at the first level, there is diversity in the modularity among the five networks. A common feature in the order parameter difference versus  $m$  is that two peaks arise, one at  $m = 4$  and the other at  $m = 16$ , indicating two hierarchical levels. Associated with each peak, clustered synchronization and community partition are optimized simultaneously.



constraint in the edge numbers, for those networks with a different modularity value at the first level, their modularity associated with the second hierarchical level assumes the identical value of 0.66. Clustered synchronization in the synthesized benchmark networks is characterized by the absolute differences in the order parameters, as shown in Fig. 10. Two peaks arise of the absolute differences: one at  $m=4$  and the other at  $m=16$ , signifying optimal clustered synchronization. In addition, when the modularity associated with the first hierarchical level increases from 0.54 to 0.77, clustered synchronization at  $m=16$  is enhanced.

## APPENDIX B: APPLICATIONS TO REAL WORLD NETWORKS

We test our dynamical evolution based method of community detection on four real world networks: coauthorship network (CAN),<sup>76</sup> dolphin social network (DSN),<sup>77</sup> book purchasing network (BPN),<sup>78</sup> and *Caenorhabditis elegans* neural network (CNN).<sup>79</sup> All network data are available from Prof. Newman's homepage (<http://www-personal.umich.edu/mejn/netdata/>). The networks and the detection results are described as follows:

### 1. CAN

The network describes the coauthorship among scientists working on network theory and experiment, with 379 nodes (authors) and 914 edges (coauthorships). The network is divided into at least 10 communities where the authors with the largest community centrality are the leaders or senior researchers of the groups working in this area.<sup>76</sup> By varying the value of  $m$ , we obtain the synchronization error matrices of nodes in different synchronous clusters used to partition the network into distinct communities via the agglomerative hierarchical tree. Note that we do not obtain the ground truth on the community structure of CAN. Instead, we compute the modularity as in Ref. 80 to evaluate and validate our community detection method. (The same approach is adopted for other three networks described below). Figure 11(a) shows the detected network modularity as a function of  $m$  and  $c$  (community number). We see that, as  $m$  is increased, the network is divided into

more communities, corresponding to larger modularity values. For the largest modularity value of 0.84 associated with  $m=34$  and  $c=23$ , we present the synchronization error matrix and the agglomerative hierarchical tree in Figs. 11(b) and 11(c), respectively. These results indicate that our nonlinear dynamical evolution based method is capable of revealing the community structure in a robust and effective fashion.

### 2. DSN

The network characterizes the social ties between dolphin pairs established by direct observation over a period of several years. The network has 62 nodes (dolphins) and 159 edges (ties). Dolphins are divided into two subgroups when a key member of the population left.<sup>77</sup> Figure 12(a) shows the modularity as a function of  $m$  and  $c$ . As  $m$  is increased, the network is divided into more communities, corresponding to larger modularity values. The largest modularity value  $Q=0.40$  occurs for  $m=4$  and  $c=5$ . Figures 12(b) and 12(c) present the synchronization error matrix and the agglomerative hierarchical tree, respectively. Except for the community with a single node, 4 smaller communities arise, which can be aggregated approximately into 2 larger ones in correspondence to the real observation.<sup>77</sup>

### 3. BPN

The network describes the co-purchasing of books by the same buyers, which has 105 nodes (books) and 441 edges (co-purchasing). The books are about the United States (US) politics published around the time of the 2004 presidential election and sold by the online bookseller Amazon.com. Figure 13(a) shows the modularity value as a function of  $m$  and  $c$ . As  $m$  is increased, the network is divided into more communities, signifying larger modularity values. The largest modularity value  $Q=0.52$  is achieved for  $m=10$  and  $c=4$ . Figures 13(b) and 13(c) present the synchronization error matrix and the agglomerative hierarchical tree, respectively, which indicates two larger and two smaller communities. Note that the emergence of two larger communities corresponds well to the existence of two major political parties for the US presidential election.

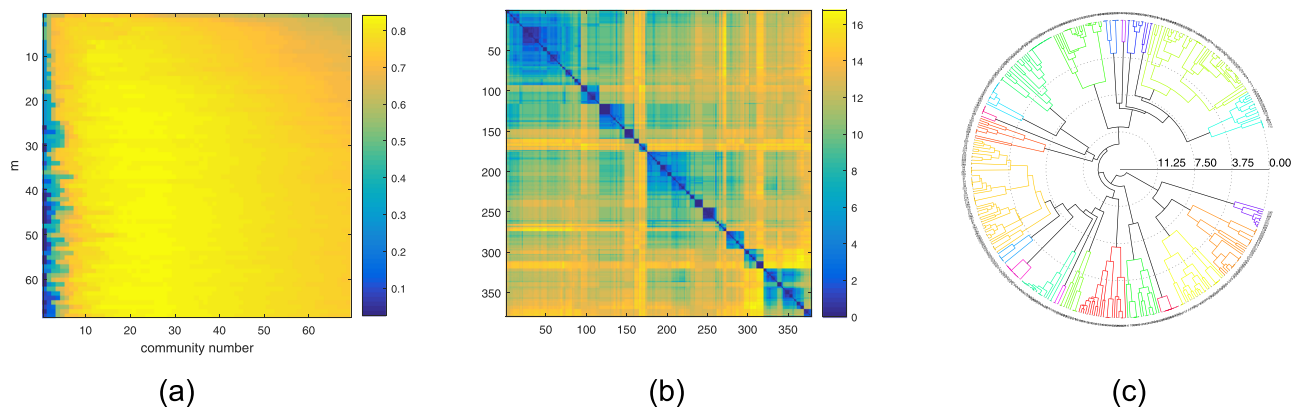


FIG. 11. Performance of the nonlinear dynamical evolution based method of community detection for the coauthorship network. (a) Modularity value as a function of  $m$  and  $c$ , (b) synchronization error matrix associated with the largest modularity value that is achieved for  $m=34$  and  $c=23$ , and (c) the polar dendrogram corresponding to (b).



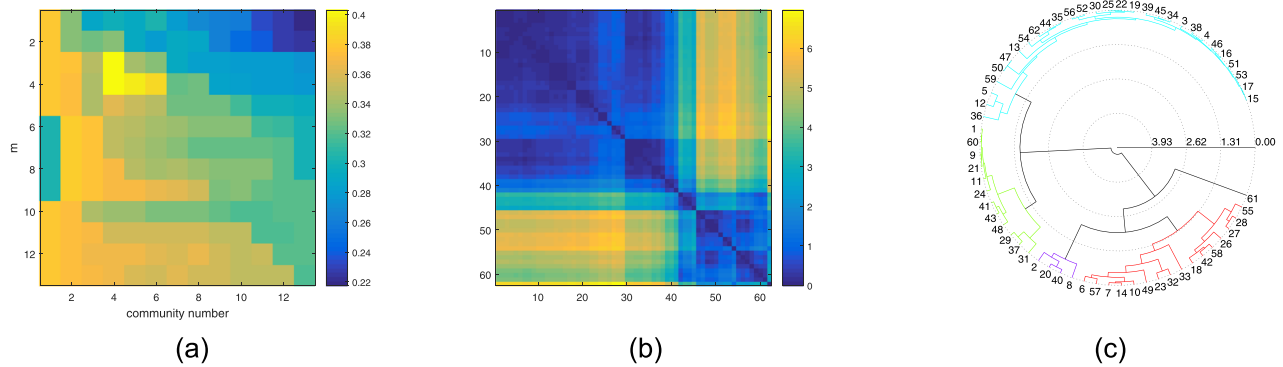


FIG. 12. Performance of the nonlinear dynamical evolution based method of community detection for the dolphin social network. (a) Modularity value as a function of  $m$  and  $c$ , (b) synchronization error matrix associated with the largest modularity value (achieved for  $m=4$  and  $c=5$ , and (c) the corresponding polar dendrogram.

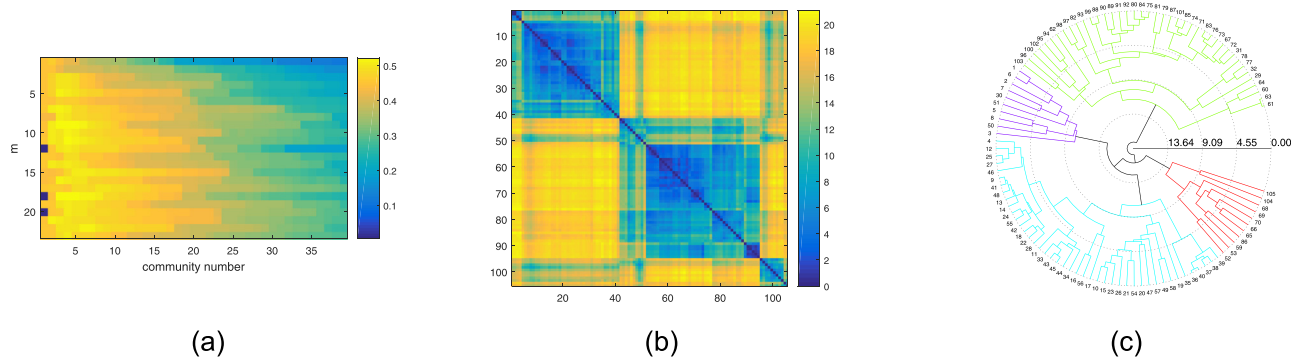


FIG. 13. Performance of the dynamical evolution based method of community detection for the political book purchasing network. (a) Modularity as a function of  $m$  and  $c$ , (b) synchronization error matrix associated with the largest modularity value achieved for  $m=10$  and  $c=4$ , and (c) the corresponding polar dendrogram.

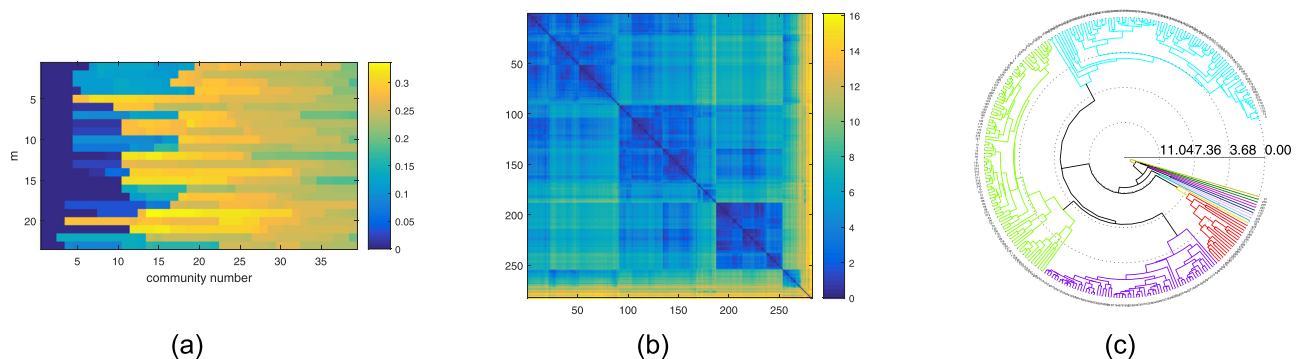


FIG. 14. Performance of the dynamical evolution based method of community detection for the *C. elegans* neural network. (a) Modularity as a function of  $m$  and  $c$ , (b) the synchronization error matrix associated with the largest modularity value achieved for  $m=20$  and  $c=15$ , and (c) the polar dendrogram corresponding to (b).

#### 4. CNN

The network tested is obtained with the nodes with one core removed from the original neural network of *C. elegans*, which has 282 nodes (neurons) and 2133 edges (neuronal wiring). Comparing with the other three networks described above, in the CNN, the nodes connect densely with each other. Figure 14(a) shows the modularity value as a function of  $m$  and  $c$ . In all cases, the modularity values are small, indicating that the CNN lacks a clear community structure. The largest modularity value  $Q=0.34$  occurs for  $m=20$  and  $c=15$ , and the corresponding synchronization error matrix

and agglomerative hierarchical tree are shown in Figs. 14(b) and 14(c), respectively. At a higher hierarchical level, clustered synchronization suggests that several larger communities may exist in the CNN.

<sup>1</sup>M. Girvan and M. E. J. Newman, "Community structure in social and biological networks," *Proc. Natl. Acad. Sci. U. S. A.* **99**, 7821–7826 (2002).

<sup>2</sup>S. Fortunato, "Community detection in graphs," *Phys. Rep.* **486**, 75–174 (2010).

<sup>3</sup>F. D. Malliaros and M. Vazirgiannis, "Clustering and community detection in directed networks: A survey," *Phys. Rep.* **533**, 95–142 (2013).

<sup>4</sup>M. E. J. Newman, *Networks: An Introduction*, 1st ed. (Oxford University Press, Oxford, UK, 2010).

- <sup>5</sup>M. E. J. Newman, "Fast algorithm for detecting community structure in networks," *Phys. Rev. E* **69**, 066133 (2004).
- <sup>6</sup>M. E. J. Newman, "Detecting community structure in networks," *Eur. Phys. J. B* **38**, 321–330 (2004).
- <sup>7</sup>R. Guimera and L. A. N. Amaral, "Functional cartography of complex metabolic networks," *Nature* **433**, 895–900 (2005).
- <sup>8</sup>L. Danon, A. Díaz-Guilera, J. Duch, and A. Arenas, "Comparing community structure identification," *J. Stat. Mech.* **2005**, P09008 (2005).
- <sup>9</sup>S. Fortunato and M. Barthelemy, "Resolution limit in community detection," *Proc. Natl. Acad. Sci. U. S. A.* **104**, 36–41 (2007).
- <sup>10</sup>V. D. Blondel, J.-L. Guillaume, R. Lambiotte, and E. Lefebvre, "Fast unfolding of community hierarchies in large networks," *J. Stat. Mech.* **2008**, P10008.
- <sup>11</sup>B. H. Good, Y.-A. de Montjoye, and A. Clauset, "Performance of modularity maximization in practical contexts," *Phys. Rev. E* **81**, 046106 (2010).
- <sup>12</sup>M. Ovelgönne and A. Geyer-Schulz, "An ensemble learning strategy for graph clustering," *Contemp. Math. Am. Math. Soc.* **588**, 187–206 (2013).
- <sup>13</sup>A. J. Alvarez, C. E. Sanz-Rodríguez, and J. L. Cabrera, "Weighting dissimilarities to detect communities in networks," *Philos. Trans. R. Soc. A* **373**, 20150108 (2015).
- <sup>14</sup>M. Rosvall and C. T. Bergstrom, "An information-theoretic framework for resolving community structure in complex networks," *Proc. Natl. Acad. Sci. U. S. A.* **104**, 7327–7331 (2007).
- <sup>15</sup>M. Rosvall and C. T. Bergstrom, "Maps of random walks on complex networks reveal community structure," *Proc. Natl. Acad. Sci. U. S. A.* **105**, 1118–1123 (2008).
- <sup>16</sup>A. Decelle, F. Krzakala, C. Moore, and L. Zdeborová, "Asymptotic analysis of the stochastic block model for modular networks and its algorithmic applications," *Phys. Rev. E* **84**, 066106 (2011).
- <sup>17</sup>B. Karrer and M. E. J. Newman, "Stochastic blockmodels and community structure in networks," *Phys. Rev. E* **83**, 016107 (2011).
- <sup>18</sup>B. Ball, B. Karrer, and M. E. J. Newman, "Efficient and principled method for detecting communities in networks," *Phys. Rev. E* **84**, 036103 (2011).
- <sup>19</sup>P. K. Gopalan and D. M. Blei, "Efficient discovery of overlapping communities in massive networks," *Proc. Natl. Acad. Sci. U. S. A.* **110**, 14534–14539 (2013).
- <sup>20</sup>T. P. Peixoto, "Eigenvalue spectra of modular networks," *Phys. Rev. Lett.* **111**, 098701 (2013).
- <sup>21</sup>T. P. Peixoto, "Parsimonious module inference in large networks," *Phys. Rev. Lett.* **110**, 148701 (2013).
- <sup>22</sup>T. P. Peixoto, "Hierarchical block structures and high-resolution model selection in large networks," *Phys. Rev. X* **4**, 011047 (2014).
- <sup>23</sup>T. P. Peixoto, "Efficient monte carlo and greedy heuristic for the inference of stochastic block models," *Phys. Rev. E* **89**, 012804 (2014).
- <sup>24</sup>G. Palla, I. Derényi, I. Farkas, and T. Vicsek, "Uncovering the overlapping community structure of complex networks in nature and society," *Nature* **435**, 814–818 (2005).
- <sup>25</sup>T. S. Evans, "Clique graphs and overlapping communities," *J. Stat. Mech.* **2010**, P12037.
- <sup>26</sup>Y.-Y. Ahn, J. P. Bagrow, and S. Lehmann, "Link communities reveal multiscala complexity in networks," *Nature* **466**, 761–764 (2010).
- <sup>27</sup>J. Reichardt and M. Leone, "(Un)detectable cluster structure in sparse networks," *Phys. Rev. Lett.* **101**, 078701 (2008).
- <sup>28</sup>A. Decelle, F. Krzakala, C. Moore, and L. Zdeborová, "Inference and phase transitions in the detection of modules in sparse networks," *Phys. Rev. Lett.* **107**, 065701 (2011).
- <sup>29</sup>R. R. Nadakuditi and M. E. J. Newman, "Graph spectra and the detectability of community structure in networks," *Phys. Rev. Lett.* **108**, 188701 (2012).
- <sup>30</sup>P. Y. Chen and A. O. Hero, "Phase transitions in spectral community detection," *IEEE Trans. Signal Process.* **63**, 4339–4347 (2015).
- <sup>31</sup>A. Clauset, C. Moore, and M. E. J. Newman, "Hierarchical structure and the prediction of missing links in networks," *Nature* **453**, 98–101 (2008).
- <sup>32</sup>R. Guimerá and M. Sales-Pardo, "Missing and spurious interactions and the reconstruction of complex networks," *Proc. Natl. Acad. Sci. U. S. A.* **106**, 22073–22078 (2009).
- <sup>33</sup>L. F. Lago-Fernandez, R. Huerta, F. Corbacho, and J. A. Siguenza, "Fast response and temporal coherent oscillations in small-world networks," *Phys. Rev. Lett.* **84**, 2758–2761 (2000).
- <sup>34</sup>P. M. Gade and C.-K. Hu, "Synchronous chaos in coupled map lattices with small-world interactions," *Phys. Rev. E* **62**, 6409–6413 (2000).
- <sup>35</sup>J. Jost and M. P. Joy, "Spectral properties and synchronization in coupled map lattices," *Phys. Rev. E* **65**, 016201 (2001).
- <sup>36</sup>M. Barahona and L. M. Pecora, "Synchronization in small-world systems," *Phys. Rev. Lett.* **89**, 054101 (2002).
- <sup>37</sup>T. Nishikawa, A. E. Motter, Y.-C. Lai, and F. C. Hoppensteadt, "Heterogeneity in oscillator networks: Are smaller worlds easier to synchronize?," *Phys. Rev. Lett.* **91**, 014101 (2003).
- <sup>38</sup>V. Belykh, I. Belykh, and M. Hasler, "Connection graph stability method for synchronized coupled chaotic systems," *Physica D* **195**, 159–187 (2004).
- <sup>39</sup>I. Belykh, M. Hasler, M. Lauret, and H. Nijmeijer, "Synchronization and graph topology," *Int. J. Bifurcation Chaos* **15**, 3423–3433 (2005).
- <sup>40</sup>M. Chavez, D.-U. Hwang, A. Amann, H. G. E. Hentschel, and S. Boccaletti, "Synchronization is enhanced in weighted complex networks," *Phys. Rev. Lett.* **94**, 218701 (2005).
- <sup>41</sup>L. Donetti, P. I. Hurtado, and M. A. Muñoz, "Entangled networks, synchronization, and optimal network topology," *Phys. Rev. Lett.* **95**, 188701 (2005).
- <sup>42</sup>C. Zhou and J. Kurths, "Dynamical weights and enhanced synchronization in adaptive complex networks," *Phys. Rev. Lett.* **96**, 164102 (2006).
- <sup>43</sup>C. Zhou and J. Kurths, "Hierarchical synchronization in complex networks with heterogeneous degrees," *Chaos* **16**, 015104 (2006).
- <sup>44</sup>K. Park, Y.-C. Lai, S. Gupte, and J.-W. Kim, "Synchronization in complex networks with a modular structure," *Chaos* **16**, 015105 (2006).
- <sup>45</sup>L. Huang, K. Park, Y.-C. Lai, L. Yang, and K. Yang, "Abnormal synchronization in complex clustered networks," *Phys. Rev. Lett.* **97**, 164101 (2006).
- <sup>46</sup>X. G. Wang, L. Huang, Y.-C. Lai, and C.-H. Lai, "Optimization of synchronization in gradient clustered networks," *Phys. Rev. E* **76**, 056113 (2007).
- <sup>47</sup>L. Huang, Y.-C. Lai, and R. A. Gatenby, "Alternating synchronizability of complex clustered networks with regular local structure," *Phys. Rev. E* **77**, 016103 (2008).
- <sup>48</sup>S.-G. Guan, X.-G. Wang, Y.-C. Lai, and C. H. Lai, "Transition to global synchronization in clustered networks," *Phys. Rev. E* **77**, 046211 (2008).
- <sup>49</sup>A. Arenas, A. Díaz-Guilera, and C. J. Pérez-Vicente, "Synchronization reveals topological scales in complex networks," *Phys. Rev. Lett.* **96**, 114102 (2006).
- <sup>50</sup>C. Zhou, L. Zemanová, G. Zamora, C. C. Hilgetag, and J. Kurths, "Hierarchical organization unveiled by functional connectivity in complex brain networks," *Phys. Rev. Lett.* **97**, 238103 (2006).
- <sup>51</sup>D. Li *et al.*, "Synchronization interfaces and overlapping communities in complex networks," *Phys. Rev. Lett.* **101**, 168701 (2008).
- <sup>52</sup>M. Li, X. Wang, and C.-H. Lai, "Evolution of functional subnetworks in complex systems," *Chaos* **20**, 045114 (2010).
- <sup>53</sup>Y. Kim, Y. Ko, and S.-H. Yook, "Structural properties of the synchronized cluster on complex networks," *Phys. Rev. E* **81**, 011139 (2010).
- <sup>54</sup>M.-Y. Zhou, Z. Zhuo, S.-M. Cai, and Z. Fu, "Community structure revealed by phase locking," *Chaos* **24**, 033128 (2014).
- <sup>55</sup>X. G. Wang, S.-G. Guan, Y.-C. Lai, B.-W. Li, and C.-H. Lai, "Desynchronization and on-off intermittency in complex networks," *EPL (Europhys. Lett.)* **88**, 28001 (2009).
- <sup>56</sup>C. Fu, H. Zhang, M. Zhan, and X. Wang, "Synchronous patterns in complex systems," *Phys. Rev. E* **85**, 066208 (2012).
- <sup>57</sup>L. M. Pecora, F. Sorrentino, A. M. Hagerstrom, T. E. Murphy, and R. Roy, "Cluster synchronization and isolated desynchronization in complex networks with symmetries," *Nat. Commun.* **5**, 4079 (2014).
- <sup>58</sup>K. Yang, X.-G. Wang, and S.-X. Qu, "Cyclic synchronous patterns in coupled discontinuous maps," *Phys. Rev. E* **92**, 022905 (2015).
- <sup>59</sup>M. T. Schaub *et al.*, "Graph partitions and cluster synchronization in networks of oscillators," *Chaos* **26**, 094821 (2016).
- <sup>60</sup>F. Sorrentino, L. M. Pecora, A. M. Hagerstrom, T. E. Murphy, and R. Roy, "Complete characterization of the stability of cluster synchronization in complex dynamical networks," *Sci. Adv.* **2**, e1501737 (2016).
- <sup>61</sup>W. Lin, H. Fan, Y. Wang, H. Ying, and X. Wang, "Controlling synchronous patterns in complex networks," *Phys. Rev. E* **93**, 042209 (2016).
- <sup>62</sup>M. De Domenico, "Diffusion geometry unravels the emergence of functional clusters in collective phenomena," *Phys. Rev. Lett.* **118**, 168301 (2017).
- <sup>63</sup>L. M. Pecora and T. L. Carroll, "Master stability functions for synchronized coupled systems," *Phys. Rev. Lett.* **80**, 2109–2112 (1998).
- <sup>64</sup>L. Huang, Q. Chen, Y.-C. Lai, and L. M. Pecora, "Generic behavior of master-stability functions in coupled nonlinear dynamical systems," *Phys. Rev. E* **80**, 036204 (2009).

- <sup>65</sup>O. E. Rössler, "Equation for continuous chaos," *Phys. Lett. A* **57**, 397–398 (1976).
- <sup>66</sup>E. N. Lorenz, "Deterministic nonperiodic flow," *J. Atmos. Sci.* **20**, 130–141 (1963).
- <sup>67</sup>U. Von Luxburg, "A tutorial on spectral clustering," *Stat. Comput.* **17**, 395–416 (2007).
- <sup>68</sup>M. Fiedler, "A property of eigenvectors of nonnegative symmetric matrices and its application to graph theory," *Czech. Math. J.* **25**, 619–633 (1975).
- <sup>69</sup>A. Davis, B. B. Gardner, and M. R. Gardner, *Deep South: A Social Anthropological Study of Caste and Class* (University of South Carolina Press, 2009).
- <sup>70</sup>W.-X. Wang, Y.-C. Lai, and C. Grebogi, "Data based identification and prediction of nonlinear and complex dynamical systems," *Phys. Rep.* **644**, 1–76 (2016).
- <sup>71</sup>M. Timme and J. Casadiego, "Revealing networks from dynamics: An introduction," *J. Phys. A: Math. Gen.* **47**, 343001 (2014).
- <sup>72</sup>J. Ren, W.-X. Wang, B. Li, and Y.-C. Lai, "Noise bridges dynamical correlation and topology in coupled oscillator networks," *Phys. Rev. Lett.* **104**, 058701 (2010).
- <sup>73</sup>W.-X. Wang, R. Yang, Y.-C. Lai, V. Kovanis, and M. A. F. Harrison, "Time-series-based prediction of complex oscillator networks via compressive sensing," *EPL (Europhys. Lett.)* **94**, 48006 (2011).
- <sup>74</sup>W.-X. Wang, Y.-C. Lai, C. Grebogi, and J.-P. Ye, "Network reconstruction based on evolutionary-game data via compressive sensing," *Phys. Rev. X* **1**, 021021 (2011).
- <sup>75</sup>M. Boguná, D. Krioukov, and K. C. Claffy, "Navigability of complex networks," *Nat. Phys.* **5**, 74–80 (2009).
- <sup>76</sup>M. E. J. Newman, "Finding community structure in networks using the eigenvectors of matrices," *Phys. Rev. E* **74**, 036014 (2006).
- <sup>77</sup>D. Lusseau *et al.*, "The bottlenose dolphin community of doubtful sound features a large proportion of long-lasting associations," *Behav. Ecol. Sociobiol.* **54**, 396–405 (2003).
- <sup>78</sup>V. Krebs, see <http://www.personal.umich.edu/mejn/netdata/> for the information about book purchasing network provided by V. Krebs.
- <sup>79</sup>D. J. Watts and S. H. Strogatz, "Collective dynamics of small-world networks," *Nature* **393**, 440–442 (1998).
- <sup>80</sup>M. E. J. Newman, "Modularity and community structure in networks," *Proc. Natl. Acad. Sci. U. S. A.* **103**, 8577–8582 (2006).